Journal of Fluids and Structures 66 (2016) 543–570

Contents lists available at ScienceDirect

Journal of Fluids and Structures

journal homepage: www.elsevier.com/locate/jfs

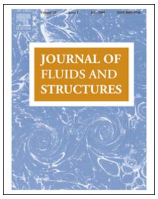

Passive aeroelastic control of a suspension bridge during erection

K.N. Bakis[a,*], D.J.N. Limebeer[a], M.S. Williams[a], J.M.R. Graham[b]

[a] *Department of Engineering Science, University of Oxford, Parks Road, Oxford OX1 3PJ, UK*
[b] *Department of Aeronautics, Imperial College London, London SW7 2AZ, UK*

ARTICLE INFO

Article history:
Received 14 January 2016
Received in revised form
29 April 2016
Accepted 29 August 2016

Keywords:
Long-span bridges
Flutter suppression
Passive aerodynamic robust control
Erection stage
Flaps
Humber bridge

ABSTRACT

This study presents a system based on passively controlled leading- and trailing-edge flaps that is designed to suppress wind-induced instabilities such as flutter and torsional divergence. The utility of the approach is demonstrated on a three-dimensional bridge model. Particular emphasis is placed on the early stages of the deck erection process when the bridge is particularly vulnerable to flutter. The flaps are activated by the deck's movements though passive phase-compensating mechanisms comprising of springs, dampers and inerters. It is demonstrated that optimised compensator parameters, and optimum hinge locations, result in a substantially improved deck aerodynamic performance. Particular importance is given to ensuring that the controlled system has good closed-loop 'robustness' properties, or in other words, that the controlled system has a high tolerance to parameter variations and uncertainties in the system dynamics. The practical use of a nonlinear optimisation algorithm with a FE bridge aeroelastic model, which includes the flap dynamics, necessitates the use of reduced-order models. A novel model reduction procedure that is based on the retention of dominant poles is introduced into the aeroelastic modelling framework. Multimodal interactions are observed at the various erection stages and conclusions are drawn with regard to the contributions of various modes of vibration to aeroelastic instabilities. The main advantage of this approach lies on the passive system's simplicity and its ability to simultaneously increase the flutter and torsional divergence boundaries. The Humber Bridge in the U.K. is chosen as a study example for numerical simulations.

1. Introduction

It is now widely appreciated that long-span bridges are prone to aerodynamic instabilities, with the iconic Tacoma Narrows bridge disaster (1940) serving as a reminder of the importance of fluid–structure interaction phenomena. This failure was a result of the gradual growth of a flutter oscillation that lasted for approximately 45 min before the bridge's failure. The spectacular collapse was attributed to the use of a structurally and aerodynamically inappropriate squat H-section for the deck's girders (Billah and Scanlan, 1991). Subsequent bridge designs, such as in the Tacoma Bridge rebuild (1950), made use of deep open-truss deck sections for increasing the bridge's torsional stiffness and enhancing its aerodynamic performance.

---

[*] Corresponding author.

http://dx.doi.org/10.1016/j.jfluidstructs.2016.08.008
0889-9746/

Nomenclature

List of symbols

A_c	cable cross sectional area (m^2)
A_d, A_l, A_t	cross section areas of the deck, leading and trailing flaps respectively (m^2)
A_g,E_g	state matrices of the generalised eigenvalue problem Eq. (14) (–)
$\tilde{A}$, $\tilde{B}$, $\tilde{C}$, $\tilde{D}$	state space realisation of the approximation of the Theodorsen function $C(s)$ (–)
$\tilde{A}_g$, $\tilde{B}_g$, $\tilde{C}_g$, $\tilde{D}_g$	matrices containing state space realisations of the approximate Theodorsen function for the N elements of the FE structure (–)
b	half chord width of the deck (m)
b	inertance in the mechanical controller realisation (kg m^2/m)
b_c	half distance between main cables (m)
B, B_g	input matrices for the state space sectional and FE model representation (–)
$C(k)$	Theodorsen function (–)
$c_l b$, $c_t b$	location of leading and trailing flap break points (m)
C_h, C_α	vertical and torsional bridge mode damping coefficient (N s/m)
C_β, C_γ	leading and trailing flap damping coefficients (N s/m)
C, C_g	output matrices for the state space sectional and FE model representation (–)
c_1,c_2	damper elements in the mechanical controller realisation ($\frac{Nmsec}{radm}$)
d_c	cable diameter (m)
d_f	flap plate thickness (m)
E	girder Young's modulus of elasticity (N/m^2)
E_c	cable Young's modulus of elasticity (N/m^2)
E_f, A_f, B_f, C_f	state space representation of the uncontrolled MIMO aeroelastic system (–)
$\tilde{E}_f$, $\tilde{A}_f$, $\tilde{B}_f$, $\tilde{C}_f$	reduced order state space representation of the uncontrolled MIMO aeroelastic system (–)
F_{se_i}	aerodynamic forces acting on a bridge finite element (N/m)
f	main cable sag (m)
G	shear modulus of elasticity (N/m^2)
$G(s)$	MIMO aeroelastic system transfer function (–)
$G_k(s)$	modal equivalent of MIMO aeroelastic system transfer function (–)
$G_\Delta(s)$	perturbed system transfer function (–)
H	horizontal cable tension (both cables) (N)
h	vertical (heave) displacement of the deck (m)
$h_{e,\min}$	length of shortest hanger length (m)
$h_e + y_e$	tower height measured from deck (m)
I_y	second moment of inertia about horizontal axis (m^4)
I_z	second moment of inertia about vertical axis (m^4)
I_a	torsional moment of inertia (m^4)
I_β, I_γ	second moment of inertias of leading and trailing flaps about their hinges (m^4)
I_m	mass moment of inertia (kg m^2/m)
k	non-dimensional reduced frequency (–)
K	MIMO controller matrix (–)
K_h, K_α	vertical and torsional bridge mode stiffnesses per unit length (kN m/m)
K_β, K_γ	leading and trailing flap retention component stiffnesses per unit length (kN m/m)
$K_l(s)$, $K_t(s)$	leading and trailing flap controllers excluding the flap retention components (–)
L	element length (m)
l_h	average hanger length or each element (m)
$L(\cdot)$	aerodynamic lift force on the deck (N/m)
l_d,t_d	parameters determining position of flap pivot points in Theodorsen and Garrick (–)
m_g	girder mass per unit length (kg/m)
m_c	mass of main cables (both cables) per unit length (kg/m)
m_e	bridge section mass per unit length (kg/m)
m_β, m_γ	mass of leading and trailing flaps per unit length (kg/m)
M, K, C	global bridge structural mass, stiffness and damping matrices (–)
M_a, K_a, C_a	global non-circulatory aerodynamic mass, stiffness and damping matrices (–)
$M_{nc,i}$, $K_{nc,i}$, $C_{nc,i}$	element non-circulatory aerodynamic mass, stiffness and damping matrices (–)
$M(\cdot)$	aerodynamic moment force on the deck (N m/m)
$M^{\beta_l}(\cdot)$, $M^{\beta_t}(\cdot)$	aerodynamic moments on the leading and trailing flaps respectively (N m/m)
$M_c^{\beta_l}(\cdot)$, $M_c^{\beta_t}(\cdot)$	feedback torques for leading and trailing flaps (N m/m)
M, υ	moment velocity pair for a one-port system (–)
$\tilde{M}$, $\tilde{N}$	normalised left coprime co-factors of $G(s)$ (–)
N	number of elements (–)
$P_{NC}(s)$	system state space representation including system dynamics and non-circulatory aerodynamic forces (–)
q	displacement vector for each element (–)
Q	displacement vector for bridge structure (–)
Q_v	velocity vector for bridge structure (–)
R_j	residue matrix corresponding to the eigen-triplet (λ_j, v_j, w_j) (–)
$R_\infty(s)$	contribution of the infinity poles at the MIMO transfer function (–)
r_b	distance from deck's rotation centre to leading flap pivot point (m)
r_{gam}	distance from deck's rotation centre to trailing flap pivot point (m)
S_α	first order moment of inertia of the deck with flap surfaces (m^3)
S_β, S_γ	first order moment of inertias of leading and trailing flaps about their hinges (m^3)
s	Laplace variable (–)
$T_{ij}(\cdot)$'s	functions defined in Theodorsen and Garrick (–)
U	mean wind velocity (m/s)
$u(s)$	output from the $C(s)$ transfer function (s)
W_{se}	weight of the suspended structure per unit